ResearchGate

See discussions, stats, and author profiles for this publication at: https://www.researchgate.net/publication/228326149

Modification of the 3d-Electronic Configuration of Manganese Phthalocyanine at the Interface to Gold

ARTICLE *in* THE JOURNAL OF PHYSICAL CHEMISTRY C · MARCH 2012

Impact Factor: 4.77 · DOI: 10.1021/Jp211445n

CITATIONS
22

READS
59

6 AUTHORS, INCLUDING:

Fotini Petraki

28 PUBLICATIONS **404** CITATIONS

SEE PROFILE

Heiko Peisert

University of Tuebingen

127 PUBLICATIONS **2,624** CITATIONS

SEE PROFILE

Thomas Chassé

University of Tuebingen

230 PUBLICATIONS **2,568** CITATIONS

SEE PROFILE

Available from: Fotini Petraki
Retrieved on: 25 January 2016

THE JOURNAL OF PHYSICAL CHEMISTRY C

Article

pubs.acs.org/JPCC

Modification of the 3d-Electronic Configuration of Manganese Phthalocyanine at the Interface to Gold

F. Petraki,*[,†] H. Peisert,[†] P. Hoffmann,[‡] J. Uihlein,[†] M. Knupfer,[§] and T. Chassé[†]

[†]University of Tuebingen, IPTC, Morgenstelle 18, 72076 Tuebingen, Germany

[‡]Helmholtz Centre Berlin for Materials and Energy, Electron storage ring BESSY II, Albert-Einstein-Str. 15, 12489 Berlin, Germany

[§]IFW Dresden, P.O. Box 270116, 01171 Dresden, Germany

ABSTRACT: The electronic structure of ultrathin films of manganese phthalocyanine (MnPc) on polycrystalline and single crystalline Au has been investigated using photoexcited spectroscopies in the lab and at synchrotron sources. Coverage-dependent photoemission and Auger spectra showed clear evidence for electronic interactions of Mn to Au at the immediate interface. Polarization-dependent N K-edge X-ray absorption spectra (XAS) supported the lying down orientation of MnPc molecular films on Au(100). The different peak features and shapes of these spectra in MnPc compared to other metal Pcs provided clear hints for hybridization with the Mn d-states of the molecule, and significant modifications of the monolayer spectra with respect to the film data indicated the involvement of these nitrogen-related states in electronic interactions at the interface. Changes of the Mn L-edge XAS spectral shape as well as the total intensity going from monolayer to multilayer coverage were detected, again indicating the local interaction of Mn d-states with substrate metal states. Resonant photoemission spectroscopy was utilized to identify valence band features with Mn character.

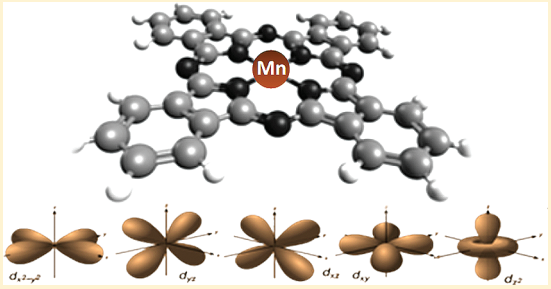

INTRODUCTION

Organic devices based on polymers and small molecules have been the subject of extensive research in both academia and industry, with the promise of large-scale, low cost, and highly efficient devices.[1−4] Furthermore, enormous progress has been made on the investigation of magnetic nanostructures, such as multilayer and thin films, revealing novel electronic and magnetic properties which are relevant for technological applications as well as for fundamental research.[5−7] Phthalocyanines are a fundamental class of organic semiconductors which can combine with almost all metal atoms in the periodic table, forming significantly stable (thermal, chemical, photochemical) complexes, with numerous applications.[8−12] Quite recently, the scientific interest has been devoted to the magnetic properties of the transition metal phthalocyanines (TMPc's) and their interaction with metallic substrates, with the aim to understand the spin configuration of these complexes and investigate their possible future applications as molecular spintronic materials in nanodevices.[13−20] The transition metals are characterized by the d-states which are successively filled across the series. The open-shell 3d ion gives rise to magnetic interactions with metallic substrates.[21−23] Among TMPc's the ferromagnetism of MnPc is rather unique and can be understood in terms of the electronic configuration of the Mn atom.[24,25] Therefore, a better understanding of the interaction between transition metal phthalocyanines/porphyrins (TPP) and metallic substrates is required. Many studies have been carried out in this direction and have shown up to now that molecule−substrate interaction occurs in many cases.[26−39] As an example XMCD studies on manganese(III)-tetraphenylporphyrin chloride on a Co substrate (MnTPPCl/Co) revealed clear evidence for exchange coupling between the organic molecules and the ferromagnetic substrate.[26] In the case of FeTPP on ferromagnetic Ni and Co films on Cu(100), a ferromagnetic coupling between Fe and Co was detected.[28] STM studies on the SnPc/Ag(111) interface have shown a π−surface and Sn−surface coupling[29] as in the case of CoPc and CoTPP on Au(111)[30−34] as well as of F_{16}CoPc on Ag(111).[35] Similar results were found also by photoemission spectroscopies (e.g., CoPc/Au,[13] CoTPP/Ag(111),[36] MPcs/Au(110),[37] etc.[35,38,39]).

In the present work, we study the interface properties between freshly evaporated ultrathin MnPc films on the surface of polycrystalline and single crystalline (100) gold substrates. A first indication for the presence of an interfacial interaction was observed in the lab by X-ray and ultraviolet photoelectron spectroscopies (XPS and UPS, respectively). This was confirmed also by synchrotron radiation based techniques such as X-ray absorption and resonant photoemission spectroscopies (XAS and ResPES, respectively). The results are discussed in comparison with the recently studied MnPc/Ag(111) interface[40] as well as the CoPc/Au(100)[41,42] and CoPc/Ag(111)[40] interfaces in terms of the 3d-states occupancy of the phthalocyanines central-metal atom.

Received: November 28, 2011
Revised: January 28, 2012

 © XXXX American Chemical Society dx.doi.org/10.1021/jp211445n | J. Phys. Chem. C XXXX, XXX, XXX−XXX

EXPERIMENTAL SECTION

The XPS and UPS measurements in the lab were performed at an ultrahigh vacuum (UHV) system equipped with a Phoibos 150 hemispherical analyzer (SPECS), a monochromatic Al Kα source, and a high-flux He discharge lamp (UVS 300, SPECS). As substrate polycrystalline gold foil was used after a sputter-cleaning procedure. XAS and ResPES were performed at the third-generation synchrotron radiation source BESSY II at the endstation UE52/PGM. The X-ray absorption spectra were recorded by measuring the sample current in both total and partial electron yield detection modes (TEY and PEY, respectively). In the case of ResPES, the energy resolution was set to about 200 meV. For the synchrotron-based measurements, a single crystalline Au(100) substrate was used after several cleaning cycles (argon ion bombardment and annealing). MnPc powder purchased by Aldrich was used after purification, and thin films were step-wisely evaporated on the clean gold substrates. The evaporation rate was monitored by a quartz crystal oscillator, and the thickness was determined by the XPS intensity ratio of the C 1s (MnPc-related) and Au 4f (substrate-related) core level lines, assuming layer over layer growth mode.

RESULTS AND DISCUSSION

I. Photoemission Spectroscopy. Investigations by photoemission spectroscopies were carried out in the lab on a polycrystalline Au substrate (foil) using conventional sources (see above). The evolution of the XPS Mn 2p core level spectra is shown in Figure 1a as a function of the organic film thickness.

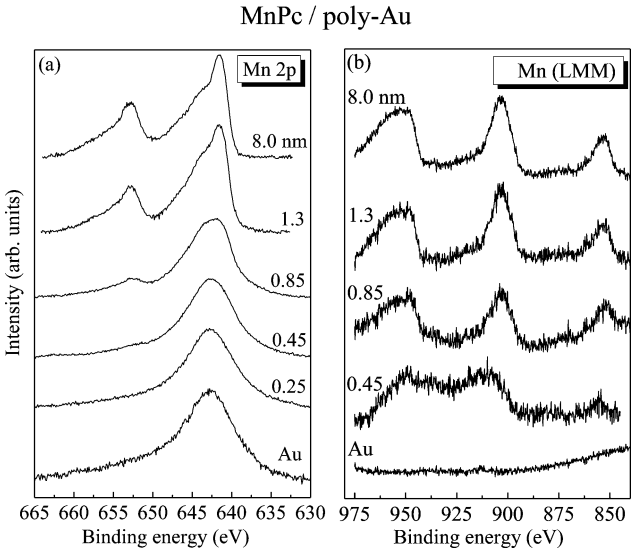

Figure 1. XPS (Al Kα) for the (a) Mn 2p and (b) Mn Auger line during the formation of the MnPc/polycrystalline Au interface.

For thicker films, the substrate characteristics are attenuated, and sharper peaks related to Mn 2p are developed. The shape and binding energy (BE) position of the Mn 2p core level spectrum for the pristine (8 nm film) MnPc are in agreement with the literature for Mn^{2+}-related XPS spectra.[39,43] Unfortunately, for MnPc on gold the Mn 2p features overlap with the broad Au $4p_{1/2}$ related peak which disables a detailed discussion of the spectral shape at the very first steps of deposition. Additionally, the fact that one monolayer (ML) of MnPc coverage corresponds to about 1/40 monolayer Mn makes it difficult to clearly distinguish different spectral features. Therefore, information on chemical shifts or possible interaction through charge transfer right at the interface with the metallic substrate can be hardly extracted only from the Mn 2p data.

To obtain more information on interactions at interfaces and on local screening effects, X-ray excited Auger electron spectroscopy (XAES) was applied. We focus on the Mn LMM (LVV) spectra to probe in particular the role of the Mn atom of the Pc. The development of Auger spectra as a function of the MnPc coverage is shown in Figure 1b. The substrate signal (bottom curve) has been subtracted from each spectrum. In general, the spectra can be described by multiplet structures arising from different coupling of final state holes. A detailed explanation of the relationship between the Auger peak shape and the electronic parameters, e.g., the function of the U/W ratio (interaction energy U between two holes and bond widths W in solids), is discussed elsewhere.[44−46] According to Figure 1b, there are clear differences in the spectral shape between the monolayer and the thick film. At low coverage (0.45 nm), the spectrum is composed of a rather broad multistructure line shape compared to the bulk-like spectrum, which can be regarded as a hint for an interaction at the interface caused by charge transfer and/or by a redistribution of the Mn electronic states (e.g., by a possible reduction of the on-site Coulomb interaction as a function of the layer thickness and/or an influence of image charges in the metallic substrate).

Another method to acquire information about interactions at interfaces is valence band photoemission (UPS). Additionally, electronic parameters of organic/metal interfaces can be determined, which are of particular importance for the performance of organic-containing electronic devices. The ionization energy (the energy difference between the HOMO leading edge and the vacuum level position) was found to be 4.5 ± 0.1 eV, significantly lower compared to other MPcs. The barrier for the injection of holes (Φ_{bh}) was found to be quite low, equal to 0.4 eV, indicating a most favorable injection in the case of the MnPc/Au interface compared to other phthalocyanine/Au interfaces (typical values for Φ_{bh} are 0.8−1.2 eV). These results are comparable to recently published data,[47] and they reveal that MnPc may exhibit exceptional interface characteristics.

A selected set of photoemission spectra in the energy region of the valence band for the Au surface and after subsequent deposition of MnPc are reported in Figure 2. After a few organic film deposition steps, the substrate-related features are strongly reduced, and MnPc-induced states appear with their maximum intensity and full development at about 1.0 nm of nominal coverage. The similarities of the valence band spectra in the BE region between 6 and 12 eV with other metal Pcs indicate that the observed photoemission features are dominated by the occupied molecular phthalocyanine ligand states.[43,47−49] The feature at about 1.0 eV of BE is related to the HOMO of the MnPc film. A detailed view of the HOMO region for increasing MnPc coverage can be seen in the middle panel of Figure 2. The HOMO of MnPc consists of a double peak, in agreement with the literature,[47] pointing to the involvement of multiple molecular levels. Differences in the HOMO region between MPcs are attributed to the occupancy of the outmost electronic 3d orbital configuration of the central metal atoms, while the excitation energy plays also a significant role in the spectral shape due to energy-dependent photoemission cross sections.[47] In particular, for MnPc, significant

dx.doi.org/10.1021/jp211445n | J. Phys. Chem. C XXXX, XXX, XXX−XXX

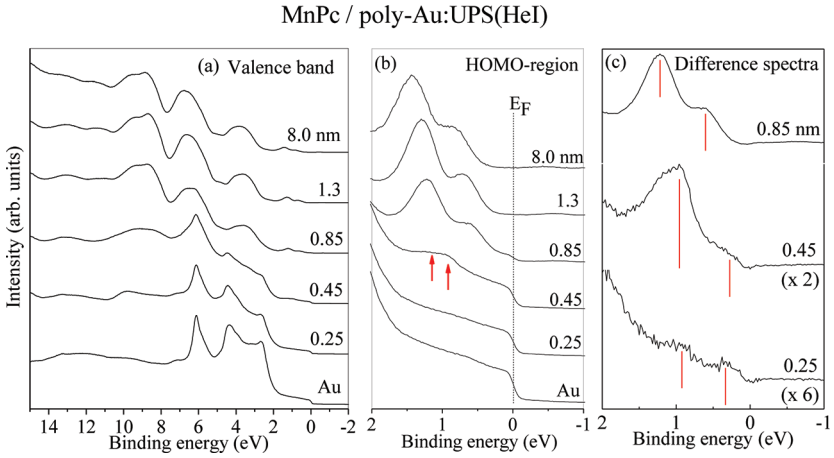

Figure 2. UPS (HeI) data from the valence band of MnPc evaporated on polycrystalline Au as a function of the coverage. Middle panel: zoom in the HOMO energy region. Right panel: the difference spectra of the HOMO region are presented after the subtraction of the Au-substrate signal.

Mn 3d contributions are predicted (see below). At submonolayer coverage, a broad feature is developed as can be seen clearly in the right panel (Figure 2c), where the HOMO region is displayed after the subtraction of the substrate signal. At a thickness of 0.45 nm, we clearly observe a splitting of the HOMO. The spectral shape at this coverage could be attributed to an interface component of the HOMO level, due to a mixing of the MnPc molecular states with the underlying metal electronic states. However, contribution from polarization effects as well as the superposition of the signal from the upper second organic layer should also be taken into consideration. These effects have been recently addressed for interfaces of metal phthalocyanines with empty or fully occupied d-shell (MgPc and ZnPc, respectively).[45] Similar behavior of the HOMO feature was recently reported for CoPc/polycrystalline Au,[13] CuPc/Au(110),[50] and CoPc, NiPc/Au(001) interfaces.[51]

II. X-ray Absorption and Resonant Photoemission. As the above presented photoemission data revealed an interface interaction between the Mn atom and the metallic substrate, further detailed investigation by synchrotron radiation based techniques is required. For this purpose, the interface between MnPc and a well-defined single crystalline Au(100) substrate was studied by XAS and ResPES.

Due to the anisotropy of the electronic properties at an organic/metal interface, the molecular ordering and orientation within the organic film are crucial for applications, thus orientation studies by X-ray absorption spectroscopy at the MnPc/Au(100) were performed. XAS monitors the resonant excitation from core levels of a specific atomic species in the material to unoccupied final states, by sweeping the photon energy of incident synchrotron light over the energy range around the absorption edges.[52] The intensity of the resonances in XAS has strong polarization dependence with the incident light, enabling the study of the molecular orientation and/or of the (unoccupied) electronic structure at a particular atomic site.

Figure 3 displays the nitrogen K-edge XAS as a function of the synchrotron light incident angle θ for an ultrathin (0.7 nm) and a multilayer (3.2 nm) MnPc film evaporated on Au(100). The first sharp absorption peaks below 405 eV of excitation energy labeled as A–D are attributed to the excitations from the N 1s core level to π^* states, while the broad absorption features at higher photon energies are assigned to transitions toward the σ^* states. According to Figure 3, the angular

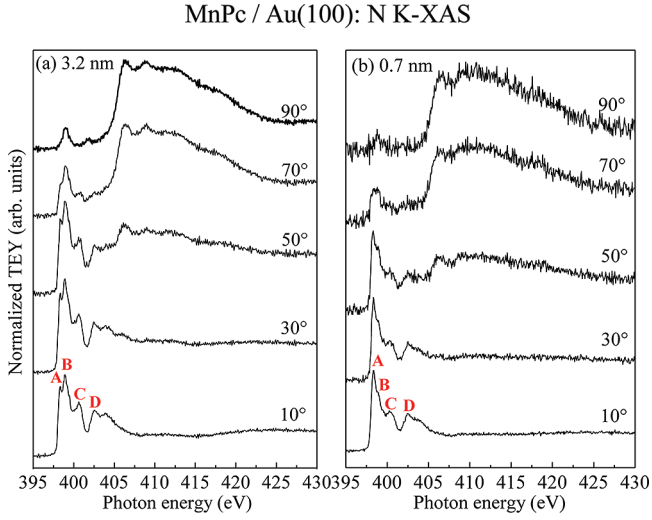

Figure 3. Angle-dependent N K-edge XAS spectra for (a) 3.2 nm and (b) 0.7 nm MnPc film deposited on Au(100).

dependence of the N-XAS spectra for both thicknesses reveals well-oriented MnPc molecules on the metallic surface. The maximum intensity of the π^* resonances is observed for grazing incidence of light and the lower for normal incidence, indicating a lying-down configuration for the MnPc molecules, in agreement with results for related systems.[40,41,59] However, some intensity in the range of the π^* resonances clearly remains at normal incidence ($\theta = 90°$) as can be seen in Figure 3a, while σ^* is completely gone at grazing incidence ($\theta = 10°$). Comparing the N K-XAS for 0.7 and 3.2 nm of MnPc coverage, certain differences are present. In particular, for the thicker film two absorption features (named as A and B) in the photon energy range between 398 and 400 eV are clearly distinguished going from grazing to normal incidence. Their intensity ratio remains almost stable (see Figure 3a). In contrast, for the 0.7 nm film, the feature A at about 398.3 eV dominates the spectra in all cases (for θ = 10°, 30°, and 50°), while feature B is significantly depressed (Figure 3b); i.e., the A/B intensity ratio is higher compared to the thicker film. The presence of these double features (A, B) at the nitrogen K-edge XAS spectra is similar to what was reported recently for the MnPc/Ag(111) interface,[40] while such a feature B is not present or resolved in the N- XAS spectra of the other studied MPcs according to the

dx.doi.org/10.1021/jp211445n | J. Phys. Chem. C XXXX, XXX, XXX–XXX

literature.[59,60] This could be regarded as a hint for the involvement of the N-atoms in an interaction with the Mn central metal atom of the Pc molecule; i.e., features A and B could be related to hybridization between unoccupied N p-states with the dπ-electronic states of the Mn central metal atom.[40]

Additional information can be acquired also by the X-ray L absorption spectra in the case of, e.g., the Mn transition metal atom. However, it should be noted here that the interpretation of the XAS L-spectra cannot be done by a simple one-electron model. Instead, all the partially empty levels of the atom contribute to the initial $3d^N$ and final $2p^5 3d^{N+1}$ states, which are strongly affected by various interactions,[40,53,54] leading to atomic-like multiplet structures. In several theoretical calculation studies the occupation of the electronic states in such systems is predicted;[22,25,53,55−58] however, the results are partially contradictory. In addition, the above-discussed spectroscopic peculiarities are often not considered, which makes a detailed understanding and explanation of the spectral shapes difficult.

Due to the rather well-defined spatial orientation of the molecules, the metal atoms are confined in a fixed configuration. The Mn L-XAS were recorded at the MnPc/Au(100) interface for both thicknesses (0.7 and 3.2 nm). As presented in Figure 4a, the general shape of the spectra in all

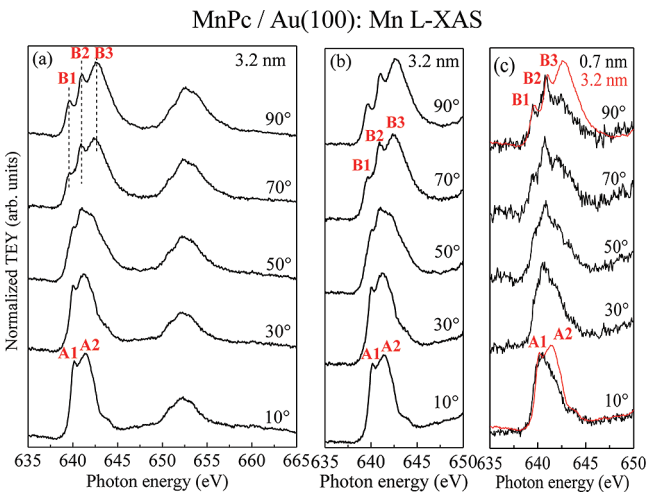

Figure 4. Angle-dependent Mn $L_{2,3}$-edge XAS spectra for (a, b) 3.2 nm and (c) 0.7 nm MnPc film deposited on Au(100) in respect to the incident light. For better comparison, the spectra for the thick film acquired at normal and grazing incidence of p-polarized light have been also included as red lines in (c).

cases is similar and representative for the Mn-related $L_{2,3}$ X-ray absorption spectrum.[40,61] It is composed of the L_3 (640−648 eV) and L_2 (650−658 eV) absorption peaks attributed to $2p_{3/2} \rightarrow 3d$ and $2p_{1/2} \rightarrow 3d$ electron transitions, respectively.[61] A clear angular dependence of the absorption features with the photon incidence and polarization is observed. If we zoom in on the L_3 peak region for the thick MnPc film (Figure 4b), we clearly see that the spectral shape is altered for different angles of incidence of the synchrotron light. In particular, the spectrum at normal incidence of light ($\theta = 90°$) is composed of a quite broad peak within which three main features can be clearly distinguished. These are B1 (639.7 eV), B2 (641.0 eV), and B3 (642.7 eV). Similarly to Mn-XAS presented previously[40] for the MnPc/Ag(111) interface, the above features arise from in-plane transitions (*xy*-polarized). The *z*-polarized transitions from the Mn $2p_{3/2}$ core level to unoccupied states (perpendicular to the molecular plane) are probed at grazing incidence ($\theta = 10°$) for the given molecular geometry. The shape of the spectrum at $\theta = 10°$ is clearly different from normal incidence ($\theta = 90°$), and it is essentially composed of two features, A1 (640.2 eV) and A2 (641.6 eV), with distinct different energetic positions compared to the B-features. With variation of the incident angle from 10° to 90°, features A1 and A2 are attenuated, and B-features are developed within the L_3 peak, which is clearly visible in Figure 4b, where we zoom in on the Mn L_3 region.

For thinner films, clear differences are observed at the Mn-XAS as displayed in Figure 4c (thickness of about 0.7 nm). For a better comparison of the data, we included also spectra for the 3.2 nm thick film (Figure 4a) in Figure 4c as red lines for selected incident angles (90° and 10°), normalized on the same step height. At grazing incidence, there is a broad peak attributed to contributions from A1 and A2, while the relative intensity of A2 is decreased compared to the thick MnPc film. At first view, the spectrum at normal incidence has a quite similar structure for both the 3.2 nm and the 0.7 nm film, where B1, B2, and B3 features are present in both cases. However, their intensities are clearly different: Whereas the B1/B2 intensity ratio is similar for both thicknesses, at about 2 ML (=0.7 nm) of coverage, the intensity of B3 is clearly significantly decreased. From the comparison of the spectra for 0.7 and 3.2 nm in Figure 4c, it can be seen that the total intensity of the whole spectra increases with the film thickness for both normal (Figure 4c, upper spectra) and grazing (Figure 4c, lower spectra) incidence, which can be attributed to the development of new features in the case of the thick film (or vice versa to the disappearance of features for molecules at the interface to the metal substrate).

Additional information about the excited states can be obtained by a qualitative analysis of the X-ray absorption spectra; in particular, the so-called branching ratio (in our case the intensity of the L_3 peak normalized by the total intensity of the Mn 2p absorption spectrum) provides information about the spin configuration of the valence electrons.[62−64] The reduced intensity for features A2 and B3 in Figure 4c for both *z*-polarized and *xy*-polarized transitions (10° and 90°) cause also a decrease of the branching ratio with decreasing film thickness, pointing to a different distribution of the d-holes of Mn in the thick organic film compared to the interface. A partial filling of the orbitals related to A2 and B3 transitions may occur at the interface, due to a charge transfer from the gold substrate toward the metal atom of the organic molecule. Thus, changes in both the Mn-related photoemission and absorption spectra can be explained via an interfacial interaction through electron withdrawing toward the Mn-3d orbitals from the metallic substrate. Most notably, spectral changes do not only affect *xy*- or *z*-polarized transitions, and therefore, the situation cannot be solely described by the filling of a particular d-orbital of Mn; the entire electronic distribution seems to change at the interface, resulting in a different multiplet structure.

The above presented results are in quite good agreement with the MnPc/Ag(111) interface,[40] even if in the case of Ag substrate the decrease of the intensity of the A2 and B3 transitions at a MnPc coverage of about 2 ML is less pronounced. An explanation for the observed small differences in Mn-XAS between the interfaces on Au and Ag could be that

dx.doi.org/10.1021/jp211445n | J. Phys. Chem. C XXXX, XXX, XXX−XXX

the interaction between wave functions of Mn and the metal substrate results in a slightly different energetic situation for both metallic substrates as recently proposed for CoPc.[40] Moreover, a different screening of the Mn 3d states may be present on the more reactive Ag substrate compared to Au, affecting local Coulomb interactions and thus the multiplet structure of the absorption spectra. Also, the determination of the film thickness in both cases is critical, and uncertainties cannot be completely ruled out. In general, however, the fact that mainly the Mn-related spectra are affected can be regarded as a proof for a charge transfer from the metal with the involvement of the partially unoccupied Mn- electronic states. In this context, the behavior is similar to recently investigated CoPc/metal interfaces,[40−42] where changes in the Co-related XAS and XPS spectra as a function of the organic coverage were more distinctive.

The electronic nature of the transitions related to the absorption features detected by XAS has been further investigated by resonant photoemission. In Figure 5, the

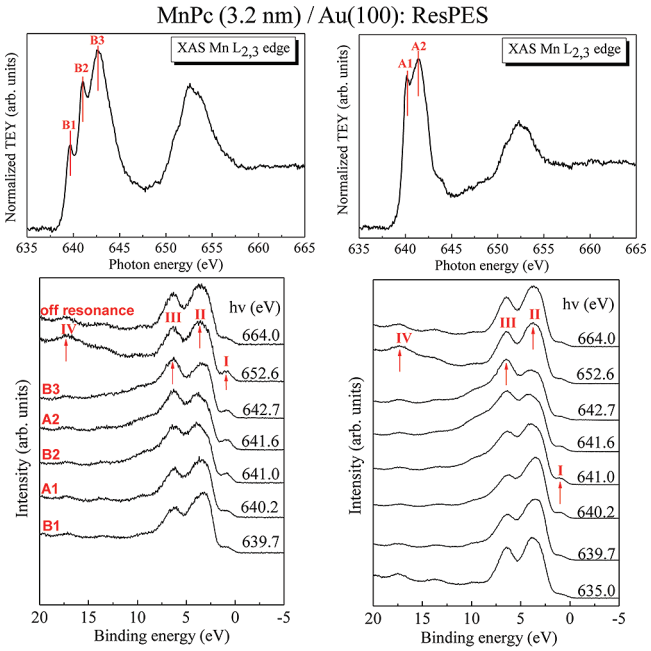

Figure 5. ResPES from a pristine MnPc film of 3.2 nm thickness deposited on Au(100) as recorded at (a) normal and (b) grazing incidence of incoming light. On the upper panel the corresponding Mn L-edge absorption spectra are displayed.

experimental valence band photoemission spectra of a 3.2 nm MnPc film evaporated on Au(100) is displayed as a function of the photon energy between 635 and 664 eV; i.e., ResPES measurements were performed in the range of the Mn L-edge to gain information about manganese-related valence band states. The spectra were recorded for both normal (Figure 5a) and grazing (Figure 5b) incidence of p-polarized light since the observed transitions in XAS are clearly angle dependent (see above). In both cases, the spectra show significant changes in shape and intensity throughout the series as highlighted by arrows in Figure 5. It is clear that particular features (referred to as I−IV) are enhanced depending on the polarization of the incident light. In general, resonant intensity enhancements are expected for those valence levels that contain substantial contributions at the core excited atomic sites (in this case the Mn). Feature I at about 1 eV is a HOMO-related peak of the organic semiconductor. For both incident angles of radiation, a strong enhancement of the HOMO region is observed for excitation energies where transitions related to the A and B XAS features occur (maybe strongest for A2 (641.6 eV), B2 (641.0 eV), and B3 (642.7 eV)), pointing to a significant contribution of the involved orbitals to the HOMO (most theoretical predictions expect Mn-related states near to the HOMO[25,58,65]). The fact that the HOMO intensity is enhanced at different geometries and at different energies induces the conclusion that different Mn 3d orbitals contribute to the HOMO related feature. This is in agreement with calculations which predict the ground state of MnPc as $(d_{xy})^1(d_\pi)^3(dz_2)^1$ (the degenerate orbitals d_{zx} and d_{yz} were often denoted as d_π).[65] The presence of holes in the *z*- as well as in the *xy*-plane may explain our experimental results. According to Nguyen et al.,[58] on the other hand, the Mn-related states near the Fermi level are mainly defined by d_{zx} and d_{yz} orbitals and to some degree by the states of p_z orbitals of the N−C bonds in the Pc's ring.[58]

In addition to the HOMO enhancement, changes in the intensity ratio between features II and III are observed in the photon energy range between 639.7 and 642.7 eV, pointing also to a contribution of Mn states. In particular, for both angles of incidence the II/III ratio decreases at the excitation energy related to A2 *z*-polarized transitions. This is better pronounced with the excitation energy where B3 transitions appear in XAS, indicating a strong localization of these Mn-related states. The structure labeled as IV is observed to be only slightly increased in BE as the photon energy increases.

Summarizing the above presented results, changes of the absorption spectral shape going from a pristine MnPc to about 2 ML were observed for MnPc on Au(100) in good agreement with the MnPc/Ag(111) interface.[40] At low coverage, a clear decrease of the relative intensity of the *xy*-polarized B3 feature is observed, revealing a (partial) filling of the corresponding state due to charge transfer. The Mn-XAS spectral features are quite broader compared to the Co-related XAS;[40−42] therefore, an additional feature as in the case of Co-XAS could be also hidden. ResPES data confirm the interaction through charge transfer, which seems to involve the Au (6s and 5d) related states located near the Fermi level, leading to an enhancement of the Mn 3d orbitals.

SUMMARY

We studied experimentally the electronic structure of Mn in MnPc in thin films and at the interface to Au. Our results indicate that different Mn 3d orbitals contribute to the HOMO related feature, in good agreement with calculations which predict a ground state of Mn in MnPc as $(d_{xy})^1(d_\pi)^3(dz_2)^1$.[65] We note, however, that the consideration of, e.g., excited states or the spin−orbit coupling may result in noninteger occupation numbers, and in particular at interfaces a coherent superposition of two charge states may occur.[23] Applying complementary spectroscopic techniques (XPS, UPS, XAS, ResPES), we found that at the MnPc/Au interface an interaction through charge transfer between the Mn-metal atom of the TMPc molecule and the substrate occurs. Changes of the Mn L-edge XAS spectra with the organic film thickness for both *xy*- and *z*-polarized transitions demonstrate that the entire electronic distribution changes at the interface to Au. Moreover, changes in the N K-XAS spectra can be regarded as a hint for the involvement of the N-atoms to the interaction at

dx.doi.org/10.1021/jp211445n | J. Phys. Chem. C XXXX, XXX, XXX−XXX

the interface due to the hybridization between unoccupied N p-states with the dπ-electronic states of the Mn-central metal atom.

AUTHOR INFORMATION

Notes

The authors declare no competing financial interest.

ACKNOWLEDGMENTS

This work has been supported financially by the German Research Council through contract number Ch 132/20-2. We acknowledge the Helmholtz-Zentrum Berlin - Electron storage ring BESSY II for provision of synchrotron radiation and for financial travel support. We want to thank W. Neu and S. Krause for technical support.

REFERENCES

(1) Morley, N. A.; Dhandapani, D.; Rao, A.; Al Qahtani, H.; Gibbs, M. R. J.; Grell, M.; Eastwood, D.; Tanner, B. K. *Synth. Met.* **2011**, *161* (7−8), 558−562.
(2) Raman, K. V.; Watson, S. M.; Shim, J. H.; Borchers, J. A.; Chang, J.; Moodera, J. S. *Phys. Rev. B* **2009**, *80* (19), 195212−1−7.
(3) Gatteschi, D; Bogani, L; Cornia, A.; Mannini, M.; Sorace, L.; Sessoli, R. *Solid State Sci.* **2008**, *10* (12), 1701−1709.
(4) Palii, A.; Tsukerblat, B.; Clemente-Juan, J. M.; Coronado, E. *Int. Rev. Phys. Chem.* **2010**, *29* (1), 135−230.
(5) Sharma, V. K.; Gupta, B. K.; Varma, G. D. *Cryst. Res. Technol.* **2011**, *46* (5), 523−528.
(6) Amiri, P.; Hashemifar, J.; Akbarzadeh, H. *Phys. Rev. B* **2011**, *83*, 165424-1−8.
(7) Werner, R.; Raisch, C.; Ruosi, A.; Davidson, B. A.; Nagel, P.; Merz, M.; Schuppler, S.; Glaser, M.; Fujii, J.; Chassé, T.; Kleiner, R.; Koelle, D. *Phys. Rev. B* **2010**, *82*, 224509-1−7.
(8) Orti, E.; Bredas, J. L. *J. Am. Chem. Soc.* **1992**, *114* (22), 8669−8675.
(9) Yamashita, A.; Hayashi, T. *Adv. Mater.* **1996**, *8* (10), 791−799.
(10) Crone, B.; Dodabalapur, A.; Lin, Y. Y.; Filas, R. W.; Bao, Z.; LaDuca, A.; Sarperhkar, R.; Katz, H. E.; Li, W. *Nature* **2000**, *403*, 521−523.
(11) Grządziel, L.; Krzywiecki, M.; Peisert, H.; Chassé, T.; Szuber, J. *Thin Solid Films* **2011**, *519*, 2187−2192.
(12) Chen, W.; Wang, L.; Qi, D. C.; Chen, S.; Gao, X. Y.; Wee, A. T. S. *Appl. Phys. Lett.* **2006**, *88*, 184102.
(13) Petraki, F.; Peisert, H.; Biswas, I.; Chassé., T. *J. Phys. Chem. C* **2010**, *114*, 17638−17643.
(14) Schuster, B. -E.; Basova, T. V.; Plyashkevich, V. A.; Peisert, H.; Chassé, T. *Thin Solid Films* **2010**, *518*, 7161−7166.
(15) Wende, H.; Bernien, M.; Luo, J.; Sorg, C.; Ponpandiard, N.; Kurde, J.; Miguel, J.; Piantek, M.; Xu, X.; Eckhold, P.; Kuch, W.; Baberschke, K.; Panchmatia, P. M.; Sanyal, B.; Oppeneer, P. M.; Eriksson, O. *Nat. Mater.* **2007**, *6*, 516−520.
(16) Bogani, L.; Wernsdorfer, W. *Nat. Mater.* **2008**, *7*, 179−186.
(17) Shen, X.; Sun, L.; Benassi, E.; Shen, Z.; Zhao, X.; Sanvito, S.; Hou, S. *J. Chem. Phys.* **2010**, *132*, 054703−1−6.
(18) Zhao, A.; Li, Q.; Chen, L.; Xiang, H.; Wang, W.; Pan, S.; Wang, B.; Xiao, X.; Yang, J.; Hou, J. G.; Zhou, Q. *Science* **2005**, *309*, 1542−1544.
(19) Kuz'min, M. D.; Hay, R.; Oison, V. *Phys. Rev. B* **2009**, *79*, 024413−1−5.
(20) Fu, Y. -S.; Ji, S. -H.; Chen, X.; Ma, X. -C.; Wu, R.; Wang, C. -C.; Duan, W. -H.; Qiu, X. -H.; Sun, B.; Zhang, P.; Jia, J. -F.; Xue, Q. -K. *Phys. Rev. Lett.* **2007**, *99*, 256601−1−4.
(21) Ehesan Ali, M. D.; Biplab, S.; Oppeneer, P. M. *J. Phys. Chem. C* **2009**, *113* (32), 14381−14383.
(22) Stradi, D.; Díaz, C.; Martín, F.; Alcamí, M. *Theor. Chem. Acc.* **2011**, *128*, 497−503.
(23) Stepanow, S.; Miedema, P. S.; Mugarza, A.; Ceballos, G.; Moras, P.; Cezar, J. C.; Carbone, C.; de Groot, F. M. F.; Gambardella, P. *Phys. Rev. B* **2011**, *83*, 220401(R)-1−4.
(24) Mitra, S.; Gregson, A.; Hatfield, W.; Weller, R. *Inorg. Chem.* **1983**, *22*, 1729−1732.
(25) Marom, N.; Kronik, L. *Appl. Phys. A: Mater. Sci. Process.* **2009**, *95*, 165−172.
(26) Scheybal, A.; Ramsvik, T.; Bertschinger, R.; Putero, M.; Nolting, F.; Jung, T. A. *Chem. Phys. Lett.* **2005**, *411*, 214−220.
(27) Javaid, S.; Bowen, M.; Boukari, S.; Joly, L.; Beaufrand, J.-B.; Chen, Xi; Dappe, Y. J.; Scheurer, F.; Kappler, J.-P.; Arabski, J.; Wulfhekel, W.; Alouani, M.; Beaurepaire, E. *Phys. Rev. Lett.* **2010**, *105*, 077201−1−4.
(28) Wende, H.; Bernien, M.; Luo, J.; Sorg, C.; Ponpandian, N.; Kurde, J.; Miguel, J.; Piantek, M.; Xu, X.; Eckhold, Ph.; Kuch, W.; Baberschke, K.; Panchmatia, P. M.; Sanyal, B.; Oppeneer, P. M.; Eriksson, O. *Nat. Mater.* **2007**, *6*, 516−520.
(29) Wang, Y.; Kröger, J.; Berndt, R.; Hofer, W. A. *J. Am. Chem. Soc.* **2009**, *131*, 3639−3643.
(30) Barlow, D. E.; Scuderiero, L.; Hipps, K. W. *Langmuir* **2004**, *20*, 4413−4421.
(31) Iancu, V.; Deshpande, A.; Hla, S. -W. *Nano Lett.* **2006**, *6*, 820−823.
(32) Gao, L.; Ji, W.; Hu, Y. B.; Cheng, Z. H.; Deng, Z. T.; Liu, Q.; Jiang, N.; Lin, X.; Guo, W.; Du, S. X.; Hofer, W. A.; Xie, X. C.; Gao, H.-J. *Phys. Rev. Lett.* **2007**, *99*, 106402−1−4.
(33) Zhao, A.; Hu, Z.; Wang, B.; Xiao, X.; Yang, J.; Hou, J. G. *J. Chem. Phys.* **2008**, *128*, 234705−1−6.
(34) Zhao, A.; Li, Q.; Chen, L.; Xiang, H.; Wang, W.; Pan, S.; Wang, B.; Xiao, X.; Yang, J.; Hou, J. G.; Zhu, Q. *Science* **2005**, *309*, 1542−1544.
(35) Toader, M.; Knupfer, M.; Zahn, D. R. T.; Hietschold, M. *Surf. Sci.* **2011**, *605*, 1510−1515.
(36) Lukasczyk, T.; Flechtner, K.; Merte, L. R.; Jux, N.; Maier, F.; Gottfried, J. M.; Steinrück, H. -P. *J. Phys. Chem. C* **2007**, *111* (7), 3090−3098.
(37) Gargiani, P.; Angelucci, M.; Mariani, C.; Betti, M. G. *Phys. Rev. B* **2010**, *81*, 085412−1−7.
(38) Ruocco, A.; Evangelista, F.; Gotter, R.; Attili, A.; Stefani, G. *J. Phys. Chem. C* **2008**, *112*, 2016−2025.
(39) Ewen, R. J.; Honeybourne, C. L. *J. Phys.: Condens. Matter* **1991**, *3*, S303−S310.
(40) Petraki, F.; Peisert, H.; Latteyer, F.; Aygül, U.; Vollmer, A.; Chassé, T. *J. Phys. Chem. C* **2011**, *115*, 21334−21340.
(41) Peisert, H.; Biswas, I.; Aygül, U.; Vollmer, A.; Chassé, T. *Chem. Phys. Lett.* **2010**, *493*, 126−129.
(42) Petraki, F.; Peisert, H.; Biswas, I.; Aygül, U.; Latteyer, F.; Vollmer, A.; Chassé, T. J. *Phys. Chem. Lett.* **2010**, *1*, 3380−3384.
(43) Nesbitt, H. W.; Banerjee, D. *Am. Mineral.* **1998**, *83*, 305−315.
(44) Fratesi, G.; Trioni, M. I.; Brivio, G. P.; Ugenti, S.; Perfetto, E.; Cini, M. *Phys. Rev. B* **2008**, *78*, 205111−1−9.
(45) Peisert, H.; Kolacyak, D.; Chassé, T. *J. Phys. Chem. C* **2009**, *113* (44), 19244−19250. Kolacyak, D.; Peisert, H.; Chassé, T. *Appl. Phys. A: Mater. Sci. Process.* **2009**, *95*, 173−178.
(46) Verdozzi, C.; Cini, M.; Marini, A. *J. Electron Spectrosc. Relat. Phenom.* **2001**, *117−118*, 41−55.
(47) Grobosch, M.; Aristov, V. Yu.; Molodtsova, O. V.; Schmidt, C.; Doyle, B. P.; Nannarone, S.; Knupfer, M. *J. Phys. Chem. C* **2009**, *113* (30), 13219−13222.
(48) Xiao, J.; Dowben, P. A. *J. Mater. Chem.* **2009**, *19*, 2172−2178.
(49) Kutzler, F. W.; Ellis, D. E. *J. Chem. Phys.* **1986**, *84* (2), 1033−1038.
(50) Evangelista, F.; Crispoldi, F.; Ruocco, A.; Betti, M. G.; Gotter, R.; Mariani, C.; Cossaro, A.; Floreano, L.; Morgante, A. *J. Chem. Phys.* **2009**, *131*, 174710−1−8.
(51) Ellis, T. S.; Park, K. T.; Ulrich, M. D.; Hulbert, S. L.; Rowe, J. E. *J. Appl. Phys.* **2006**, *100*, 093515−1−10.
(52) Chen, W.; Wee, A. T. S. *J. Electron Spectrosc. Relat. Phenom.* **2009**, *172* (1−3), 54−63.

(53) Kroll, T.; Aristov, V. Yu.; Molodtsova, O. V.; Ossipyan, Yu. A.; Vyalikh, D. V.; Buechner, B.; Knupfer, M. *J. Phys. Chem. A* **2009**, *113*, 8917−8922.
(54) de Groot, F. M. F. *Coord. Chem. Rev.* **2005**, *249*, 31−63.
(55) Grobosch, M.; Schmidt, C.; Kraus, R.; Knupfer, M. *Org. Electron.* **2010**, *11* (9), 1483−1488.
(56) Li, F.; Zhenga, Q.; Yanga, G.; Lu, L. *Dyes Pigm.* **2008**, *77* (2), 277−280.
(57) Liao, M. S.; Scheiner, S. *J. Chem. Phys.* **2001**, *114* (22), 9780−9791.
(58) Nguyen, T. Q.; Escano, M. C. S.; Kasai, H. *J. Phys. Chem. B* **2010**, *114*, 10017−10021.
(59) Peisert, H.; Biswas, I.; Knupfer, M.; Chassé, T. *Physica Status Solidi B* **2009**, *246*, 1529−1545.
(60) Huang, H.; Chen, W.; Chen, S.; Qi, D. C.; Gao, X. Y.; Wee, A. T. S. *Appl. Phys. Lett.* **2009**, *94*, 163304−1−3.
(61) Kawai, J.; Mizutani, Y.; Sugimura, T.; Sai, M.; Higuchi, T.; Harada, Y.; Ishiwata, Y.; Fukushima, A.; Fujisawa, M.; Watanabe, M.; Maeda, K.; Shin, S.; Gohshi, Y. *Spectrochim. Acta, Part B* **2000**, *55*, 1385−1395. Siemeling, U.; Schirrmacher, C.; Glebe, U.; Bruhn, C.; Baio, J. E.; Arnadottir, L.; Castner, D. G.; Weidner, T. *Inorg. Chim. Acta* **2011**, *374*, 302−312.
(62) Van der Laan, G. *J. Electron Spectrosc. Relat. Phenom.* **1997**, *86*, 41−47.
(63) Thole, B. T.; Van der Laan, G.; Butler, P. H. *Chem. Phys. Lett.* **1988**, *149* (3), 295−299.
(64) Goering, E. *Philos. Mag.* **2005**, *85* (25), 2895−2911.
(65) Liao, M. S.; Watts, J. D.; Huang, M. *J. Inorg. Chem* **2005**, *44*, 1941−1949.